HHS Public Access

Author manuscript

Sci Transl Med. Author manuscript; available in PMC 2021 October 28.

Published in final edited form as:

Sci Transl Med. 2020 October 28; 12(567): . doi:10.1126/scitranslmed.abb7656.

A modified drug regimen clears active and dormant trypanosomes in mouse models of Chagas disease

Juan M. Bustamante[1,†], **Fernando Sanchez-Valdez**[1,2,†], **Angel M. Padilla**[1], **Brooke White**[1], **Wei Wang**[1], **Rick L. Tarleton**[1,3,*]

[1]Center for Tropical and Emerging Global Diseases, University of Georgia, Athens

[2]Instituto de Patología Experimental, Universidad Nacional de Salta-CONICET, Salta, Argentina

[3]Department of Cellular Biology, University of Georgia, Athens

Abstract

A major contributor to treatment failure in Chagas disease, caused by infection with the protozoan parasite *Trypanosoma cruzi*, is that current treatment regimens do not address the drug-insensitivity of transiently dormant *T. cruzi* amastigotes. Here, we demonstrated that use of a currently available drug in a modified treatment regimen of higher individual doses given less frequently over an extended treatment period, could consistently extinguish *T. cruzi* infection in three mouse models of Chagas disease. Once per week administration of benznidazole at a dose 2.5-5 times the standard daily dose rapidly eliminated actively replicating parasites and ultimately eradicated the residual, transiently dormant parasite population in mice. This outcome was initially confirmed in 'difficult to cure' mouse infection models using immunological, parasitological, and molecular biological approaches and ultimately corroborated by whole organ analysis of optically clarified tissues using light-sheet fluorescence microscopy (LSFM). This tool was effective for monitoring pathogen load in intact organs, including detection of individual dormant parasites, and for assessing treatment outcomes. LSFM-based analysis also suggested that dormant amastigotes of *T. cruzi* may not be fully resistant to trypanocidal compounds such as benznidazole. Collectively these studies provide important information on the phenomenon of dormancy in *T.*

*To whom correspondence should be addressed, tarleton@uga.edu.

†These authors contributed equally to this work.

Authors contributions: Juan M. Bustamante, Conceptualization, Formal analysis, Investigation, Methodology, Writing original draft, Funding acquisition; Fernando J Sanchez-Valdez, Conceptualization, Formal analysis, Investigation, Methodology, Writing original draft; Angel Padilla, Conceptualization, Formal analysis, Investigation, Methodology, Writing review and editing; Wei Wang, Investigation, Methodology, Writing original draft; Brooke White, Investigation, Methodology; Rick L Tarleton, Conceptualization, Supervision, Funding acquisition, Methodology, Writing—original draft, Project administration, Writing—review and editing. Juan M. Bustamante performed mice infections, in vivo imaging, drug treatment, hemocultures, T cell phenotype, flow cytometry analysis and perfusion and tissue collection assays. Fernando Sanchez Valdez performed tissue clarification, confocal laser-scanning microscopy imaging, light-sheet fluorescent microscopy and image processing as well as analysis and data acquisition on fluorescent microscopy. Angel Padilla performed mice infections, perfusion and tissue collection assays and analysis of data. Wei Wang carried out the in vitro maximal luminescence ATP detection assay. Brooke White performed quantitative polymerase chain reaction and hemoculture.

Related resources:
DOI: 10.1126/scitranslmed.aax4204
DOI: 10.1126/scitranslmed.aac5477
DOI: 10.1126/scitranslmed.aaa3043

Competing interests: The Authors declare no competing interests.

Data and materials availability:
All data associated with this study are present in the paper or the supplementary materials.

cruzi infection in mice, demonstrate methods to therapeutically override dormancy using a currently available drug, and provide methods to monitor alternative therapeutic approaches for this, and possibly other, low density infectious agents.

One Sentence Summary:

A modified regimen of benznidazole prevents *Trypanosoma cruzi* dormancy-dependent treatment failure in several mouse models of Chagas disease.

Introduction

Chagas disease, caused by the protozoan parasite *Trypanosoma cruzi*, is a potentially life-threatening infection that currently affects at least 6 million people in the Americas and has spread to non-endemic countries through human migration (1–3). The number of individuals infected with *T. cruzi* continues to increase and is amplified by a widespread failure to apply vector control approaches and the absence of effective vaccines. Furthermore, the disease symptoms are exacerbated by the fact that most infections with *T. cruzi* go undetected and/or untreated. The frontline therapies for *T. cruzi* infection consist of two compounds, benznidazole (BNZ) and nifurtimox (NFX), both of which are associated with adverse events, have unpredictable efficacy and are administered in an intense, twice-daily regimen for 30-60 days (4–6). These attributes lead to treatment interruption in approximately 20% of individuals (6, 7), and contribute to the fact that only ~1% of infected subjects are thought to receive a full course of treatment (8). This situation is particularly dire since *T. cruzi* infection rarely resolves without treatment and often progressively damages critical organs such as the heart, leading to eventual heart failure.

The frequent failure of the standard 30-60 day BNZ treatment regimens is paradoxical, given that a single in vivo dose of this compound rapidly reduces parasite load by ~90% (9) and that shortened treatment regimens in experimental animals and humans occasionally are curative (7, 10). One facet of the inconsistency in treatment outcomes is *T. cruzi* strain variation, as some isolates are more resistant to BNZ-induced clearance in vivo (9, 10), despite having similar sensitivity to BNZ in vitro. Indeed, there are major gaps in our understanding of the biology of intracellular amastigotes of *T. cruzi*, the targets for drug therapy. *T. cruzi* amastigotes replicate in the cytoplasm of a wide variety of host cell types but the true tissue distribution in vivo, the kinetics of replication in different host cell and tissue types and the impact of host factors, including immune effectors, on parasite control and persistence, are not known. We recently reported a previously undescribed stage in the intracellular lifecycle of *T. cruzi*, transiently dormant, and non-replicating amastigotes that are resistant to treatment with existing trypanocidal compounds, including BNZ (9). The transition into dormancy by *T. cruzi* amastigotes occurs at a very low frequency and appears to be stochastic and not a response to stressors, including drug exposure. This dormancy phenotype is also transient, with formally dormant amastigotes returning to an active dividing state that is sensitive to drug. Thus, trypanocidal drugs very efficiently kill actively dividing amastigotes but not dormant forms, suggesting that dormancy is a primary cause of the failure of these drugs to achieve consistent parasitological cure in this and perhaps other parasitic infection (11).

These new findings reveal a need to rethink drug discovery for Chagas disease. To date, all screens for anti-*T. cruzi* compounds have focused on discovering new entities that kill actively dividing/non-dormant amastigotes. New screens capable of identifying compounds that can interrupt or reverse dormancy or kill dormant forms are needed. Alternatively, we can ask how we might better apply the existing trypanocidal compounds to overcome dormancy. Based on the knowledge that single doses of BNZ are highly toxic for replicating *T. cruzi* and with the assumption that dormancy is time-limited, in this study we have developed and evaluated a longer-term but less-intensive and ultimately drug-sparing BNZ treatment protocol in mice with chronic infections with hard-to-cure isolates of *T. cruzi*. Further, to document the kinetics and impact of this protocol in vivo over time, we established tissue-clearing and light-sheet fluorescent microscopy (LSFM) methods that allow the quantification of actively replicating and dormant parasites – including single parasites – in intact tissues and organs. Application of these regimens and methodologies provide new insights on dormancy in *T. cruzi* and suggest methods to achieve parasitological cure despite dormancy.

Results

Single or multiple intermittent doses of BNZ sustainably reduce parasite load

Following on our new understanding of the resistance of dormant amastigotes to BNZ and other trypanocidal drugs, and solid evidence for the failure of current, intensive drug-treatment protocols in Chagas disease, we hypothesized that delivering BNZ over a longer period of time could “outpace” dormancy, killing all actively replicating parasites early in the treatment regimen and eventually clearing all parasites, as the remaining dormant forms gradually emerged over time of treatment. Given the known toxicity of the daily BNZ treatment protocols (6, 12, 13), extending daily dosing for >60 days seemed impractical. However, evidence of the substantial impact of intermittent dosing once every ~5 days) on *T. cruzi* infection in humans and experimental animals (7, 10) provided support for a protocol of less frequent dosing. To examine directly the impact of intermittent dosing on total parasite load, we monitored luciferase-expressing parasites at the site of infection after the standard daily oral dose of 100 mg/kg BNZ or a 5-fold higher dose (Fig. 1A).

Both the 100 and 500 mg/kg BNZ doses reduced parasite numbers by >90% within 1 day after treatment, as expected (9) (Fig. 1B and C). However, the 500 mg/kg dose had a sustained impact for at least 5 days while parasite numbers in mice treated with 100 mg/kg began to increase within 2 days after treatment. The differential impact of the two BNZ doses on parasite load was confirmed by quantitative PCR (qPCR) detection of parasites in the footpad of wild-type mice 5 days after a single BNZ treatment (Fig. 1D). In both cases, subsequent doses of BNZ drove parasite numbers even lower and 2-3 doses over ~20 days at either dose was sufficient to reduce parasite load to background (Fig 1C) in these IFN-gamma-deficient mice that are otherwise unable to control infection without drug intervention (14, 15). These results demonstrate that less frequent BNZ dosing has a durable impact on parasite numbers but the standard dose of 100mg/kg BNZ was initially less effective at decreasing and maintaining a reduced parasite load when used intermittently.

Once-per-week treatment with BNZ achieves parasitological cure

We then carried out a large-scale treatment study using mice chronically infected with the ARC-0704 line, a strain of *T. cruzi* that, like the Colombiana used in the experiments in Figure 1, is relatively resistant to BNZ-induced cure using the standard 40-day treatment protocol (fig. S1). Mice were treated weekly with either 100 or 500 mg/kg beginning at 120 days post-infection and the length of treatment was not initially defined (an open-ended protocol; Fig. 2A). Because parasite load in mice with chronic *T. cruzi* infection – even without treatment - is generally assessable only by highly sensitive protocols like qPCR detection of parasite DNA in tissues at necropsy (16, 17), we were unable to measure directly parasite numbers during the course of this treatment study. However, in cured infections, we had previously shown that the memory status of *T. cruzi*-specific $CD8^+$ T cells, indicating whether they had recently encountered *T. cruzi* antigen, could serve as a dependable indicator of cure (10, 18). Thus, we used the frequency of the IL-7 receptor alpha (CD127) high, *T. cruzi*-specific $CD8^+$ T cells (termed *T. cruzi*-specific T_{cm}) as a surrogate for parasite load over the treatment course.

Mice receiving weekly doses of BNZ of either 100 mg/kg or 500mg/kg exhibited increased frequencies of $CD127^+$ *T. cruzi*-specific $CD8^+$ T cells in the blood, suggestive of reduced parasite load. By 35 weeks post-treatment, the percentage of these *T. cruzi*-specific T_{cm} had plateaued in all groups (Fig. 2B), but with a clear difference between the 2 treated groups with mice in the high dose group reaching average percentages of 60-85% T_{cm} among the *T. cruzi*-specific ($TSKB20^+$) $CD8^+$ T cells while mice in the 100mg/kg group on average achieved percentages of 35-45% T_{cm}. Untreated mice maintained *T. cruzi* - specific T_{cm} percentages near 20% as previously reported (10, 18, 19). qPCR measurement of *T. cruzi* DNA in tissues taken at 37 weeks of treatment from a subset of animals with the highest *T. cruzi* -specific T_{cm} in the 2 treated groups (Fig. S2A and B) confirmed that *T. cruzi*-specific T_{cm} accurately reflected parasite load and further demonstrated that the mice from the 500 mg/kg treatment group were all parasite-free by week 37 (Fig. S2C and D). Hemocultures also confirmed the persistence of infection in untreated mice and its absence in the mice treated weekly with 500 mg/kg BNZ for 37 weeks.

These results suggested that mice in the 500 mg/kg treatment group were cured after 37 weeks of treatment but that those in the 100 mg/kg group might be a mixture of cured and not-cured. To further explore this conclusion, we modified the treatment protocol in the remaining mice at the 50 week mark, increasing or decreasing the treatment dose or stopping treatment altogether (Fig. 2A), and monitored the impact on *T. cruzi* -specific T_{cm} (Fig. 2B) and ultimately on parasite burden in tissues by qPCR (Fig. 2C). For the 500 mg/kg group, we initially lowered the weekly treatment dose to 100 mg/ml. The frequency of *T. cruzi* -specific T_{cm}, remained high after this change, and indeed after stopping treatment completely at 55 weeks (Fig. 2B). When the experiment was terminated at 77 weeks post-initiation of treatment (approximately 94 weeks of infection), qPCR analysis of tissues (Fig. 2C) and hemoculture of blood (Fig. 2D) from these mice confirmed the absence of infection. The mice treated at 100 mg/kg were split into 3 groups. In the group in which treatment was stopped at 50 weeks, the numbers of *T. cruzi* -specific T_{cm} reverted to that of mice who never received treatment and 100% of these mice had detectable parasites in tissues at 77

weeks post-treatment initiation (Fig. 2B and C). The group remaining on 100 mg/ml BNZ maintained an intermediate frequency of *T. cruzi* -specific T_{cm} as did mice moved from 100 mg/kg to 500 mg/kg treatment for >20 weeks and both of these groups contained multiple animals with detectable parasite load at the termination of the experiment at week 77 (Fig. 2C). Notably, parasites recovered from mice treated with 100mg/kg of BNZ for 55 weeks (100w/STOP) were equally susceptible to BNZ in vitro as those isolated from untreated mice (Fig. S3), indicating that the failure of this treatment regimen to resolve the infection was not due to induction of classical drug resistance. Collectively, this study showed that mice receiving a weekly dose of 500 mg/kg BNZ for as few as 37 weeks were uniformly cured of chronic *T. cruzi* infection with a "BNZ-insensitive" strain. However weekly treatment at the normal daily BNZ dose of 100mg/kg failed to dependably resolve the infection, even after up to 1.5 years of treatment.

Weekly dosing at 2.5-5X the daily dose for 30 weeks cures chronic *T. cruzi* infection

The design of the decreased frequency/extended period treatment protocol validated in the experiments above is based upon the premise that the total treatment period has to extend beyond the maximum length of amastigote dormancy in order to be effective. Our surrogate marker for parasitological cure – the frequency of *T. cruzi* -specific T_{cm} - plateaued at ~15 weeks of treatment with 500 mg/kg/wk (Fig. 2B), establishing a potential minimal treatment period for cure. To define better the minimum treatment period needed to overcome dormancy, we initiated a weekly treatment experiment with discrete endpoints of 20 and 30 weeks. This experiment used a second "difficult to cure" *T. cruzi* strain, the Colombiana (10), in order to test the broader applicability of this dosing approach and we included an intermediate dose group of 250 mg/kg as a dose-sparing test (Fig. 3).

Although the numbers and kinetics of *T. cruzi* -specific T_{cm} in the Colombiana infection are slightly different from that in the ARC-0704-infected mice in Figure 2, as expected, the numbers of T_{cm} rose after initiation of the weekly BNZ treatment, reaching an average of ~60% in all treated groups by 20 weeks of treatment (Fig 3). However, qPCR analysis of tissues revealed that a proportion of mice in both the 250 mg or 500 mg/kg/wk groups, were still infected when assayed immediately after (Fig 3A and D) or 25 weeks after (Fig 3B and E) the 20 week treatment regimen. Extending the treatment to 30 weeks achieved cure in 100% of animals in both treatment groups based upon qPCR (Fig 3C and F) and hemoculture (8 of 8 samples parasite negative in treated groups and 6 of 6 samples *T. cruzi* positive in the untreated group). Thus, 30 weekly doses of either 250 or 500 mg/kg BNZ (2.5-5X the conventional daily dose) is sufficient to obtain consistent parasitological cure in mice chronically infected with *T. cruzi* strains that are relatively resistant to cure using conventional, daily treatment regimens.

Light-sheet fluorescence microscopy detects *T. cruzi*-infected cells in intact tissues and organs

The above data supported our previous observations that BNZ was highly effective in rapidly killing actively dividing *T. cruzi* but apparently ineffective against dormant parasites, and the success of the extended (~30 week) treatment protocol in curing *T. cruzi* infection was consistent with an upper limit of ~30 weeks for *T. cruzi* amastigotes to remain dormant.

However direct, in vivo confirmation of these conclusions was impossible to obtain with previous approaches such as in vivo imaging, standard histology or qPCR of tissue samples. We adopted CUBIC tissue clarification protocols (20), and used Light-Sheet Fluorescence Microscopy (LSFM) (21, 22) technology coupled to 3D organ reconstruction and automated quantification to visualize and track fluorescent protein (FP)-expressing *T. cruzi* in whole mouse organs. This approach allowed detection of *T. cruzi* not only in tissues of IFN-gamma–deficient mice (Fig. 4A and B and Movies 1 and S1) but also in tissues of wild-type mice, including individual parasites in chronically infected tissues where parasites are very sparse (Fig. 4C, and Movie 2). A wide range of tissues were amenable to clarification and LSFM imaging (Fig. S4). Although individual parasites could not be resolved in heavily infected cells (often referred to as “nests”) by this LSFM approach, Confocal Laser-Scanning Microscopy (CLSM) of thin sections of the same clarified tissues confirmed the identification of *T. cruzi*-infected cells (Fig. 4D–E). Supporting the results in Figure 1, LSFM allowed us to detect the near complete clearance of parasites in the heart following 2 daily doses of BNZ (Fig. 4F and Movie S2). LSFM also permitted the monitoring of immune-mediated control of tissue parasite load over time in whole organs, and for the first time, suggested a differential timing of parasite control in different tissues (Fig. 4G).

Weekly dosing with BNZ eventually clears both actively replicating and dormant amastigotes from tissues.

We next utilized tissue clarification coupled to LSFM to further assess the in vivo activities of BNZ ascertained from the earlier infection/treatment studies, in intact tissues and organs. We infected mice with the Colombiana strain of *T. cruzi* expressing tdTomato and then starting at 5 dpi, treated with either 100 or 500 mg/kg/week over a period of 7 weeks. As expected, parasites became extremely rare in heart and skeletal muscle early in the treatment protocol in mice in both dosing groups, with fewer than 5 parasites or parasite nests per tissue (Fig. 5). However, following 6-8 weekly doses, no parasites were detected in heart and skeletal muscle of mice treated with 500 mg/kg of BNZ whereas mice in the 100 mg/kg group continued to exhibit a very low, but routinely detectable number of *T. cruzi*-infected cells.

Collectively, these results confirmed the efficacy of higher dose (500 mg/kg) weekly BNZ treatments in drastically reducing parasite load in mice and largely support the conclusions from immunological surrogates and qPCR and hemoculture-based methods of detection of parasite persistence as shown in Figures 1 and 2. These results also suggested that the higher dose weekly treatment regimen was eventually clearing dormant parasites while the lower dose treatment was not. To directly address this point, we infected mice with the tdTomato-expressing and DiR near-infrared cyanine dye-stained trypomastigotes of the Colombiana strain of *T. cruzi*. The use of the DiR fluorescent dye allows us to track dormant parasites by visualizing those that had not diluted the dye as a result of replication (as shown for CellTrace Violet in our previous studies (9)). We first confirmed that DiR fluorescence survived the CUBIC clearing process (Fig S7). Surprisingly, mice treated weekly at 500 mg/kg of BNZ showed loss of both replicating and non-replicating (dormant) amastigotes in heart, skeletal muscle and intestine within 6 weeks (Fig. 6 A–C, Movie 3 and Table S1)

whereas mice receiving the 100mg/kg dosage over 11 weeks had persistent actively dividing and dormant parasites in these tissues (Table S2).

Discussion

Chagas disease is a progressive disease caused by persistent infection with *T. cruzi* and prevention of this disease almost certainly requires sterile parasitological cure; simply reducing parasite burden does not prevent disease progression. For this reason, the recent identification of dormancy in *T. cruzi* amastigotes is particularly concerning as there is a dearth of information on the mechanism of this process, and current drugs appear to have modest, if any effect on the dormant stages. A number of long-used (BNZ and NFX) and other initially promising new candidates with potent in vitro anti-*T. cruzi* activity (23–26), routinely fail to cure infection, and this failure is at least in part due to the lack of impact of these compounds on dormant forms.

The recognition of dormancy as a factor in treatment failure also provides a path for improving treatment efficacy through specifically targeting dormant forms. In this study, we identified a treatment protocol that uses a readily available, FDA-approved compound in a rationally designed regimen that consistently provided sterile parasitological cure. This outcome was achieved under the most rigorous infection conditions, using “difficult to cure” parasite strains and established, chronic infections and was validated using previously authenticated immunological and parasitological protocols and further, with a newly established tissue clearing/LSFM approach that allows detection of host cells containing individual, including dormant, amastigotes in whole organs.

The high-dose, extended-time protocol evaluated in this study considered characteristics of *T. cruzi* infection that were not appreciated when the standard daily administration protocol was developed nearly 50 years ago, and its success depended on both extending the BNZ treatment period (to 30 weeks) and increasing each dose to at least 2.5X what is normally used in daily dosing regimens. The extended treatment period may be necessary to challenge the stochastic nature of dormancy in *T. cruzi* (9, 10). The successful cure using a 30-week (but not 20 week) treatment regimen in chronically infected mice indicates that the ability of amastigotes to remain quiescent is time-limited.

The absolute requirement for a higher dose of BNZ in this protocol became evident from the rapid rebound in parasite growth after a single standard (100 mg/kg) dose of BNZ (Fig. 1), and was confirmed by the evidence of persisting parasites in tissues by LSFM and by qPCR in mice treated for as long as 1 year at this dose. In contrast, mice receiving 2.5 – 5X the standard BNZ dose showed clearance of both actively dividing and (eventually) non-dividing amastigotes, establishing that insufficient dosing for BNZ is a second factor in the frequent failure of current protocols, which needs to be reconsidered in all species.

The two variables of BNZ dose and length of treatment have not previously been thoroughly evaluated in concert in *T. cruzi* infection. However, because the higher BNZ dosage has a sustained impact on actively replicating *T. cruzi* (despite a half-life of ~12 hrs in mice (27, 28)) it is possible to both increase the dose of BNZ and extend the length of treatment using

~1/3rd the weekly dose of standard protocols while only marginally increasing total cumulative exposure over the 30 week treatment period, relative to the conventional 60 day, daily treatment course.

A limitation of our study is that the dosing regimen was evaluated only in mice. However mice have proven to be extremely reliable indicators of drug efficacy (and other aspects) in Chagas disease, when appropriately utilized and carefully evaluated (9, 10, 18, 29). The length of treatment is also a disadvantage of this new protocol as is the higher bolus with each treatment, which could increase the potential for toxicity although we observed no toxicity of these regimens in mice. Additional modifications – such as twice weekly dosing - might shorten the treatment period but also risks increasing side effects. On ongoing studies in dogs and non-human primates should be informative on these points.

A surprising finding using LSFM to monitor the attrition of dye-positive dormant amastigotes over time is that these dormant amastigotes declined more rapidly in mice under weekly BNZ treatment than in untreated mice. This is counter to our interpretation of previous studies (9), and suggests that dormant parasites are not totally refractory to BNZ treatment, particularly at the higher doses used in this protocol, an encouraging hint that dormant *T. cruzi* are accessible to some compounds. Furthermore, the very rapid and highly efficient clearance of actively replicating *T. cruzi* with one dose of BNZ suggests that if combined with a compound that rapidly reverses *T. cruzi* dormancy, a completely curative treatment requiring only a few days of treatment – perhaps even with a single combined dose – could be developed.

Lastly, this study introduces new protocols to quantify both actively dividing and individual dormant parasite in intact tissues and organs. Assessment of parasite numbers using LSFM of clarified tissues should be integrated into protocols for comparison of therapeutic regimens and assessment of new candidate drugs and variations on this basic technique will be useful in understanding parasite behavior in vivo, immune responses to parasites, and generation of tissue damage - issues that have previously been approached only via highly selective sampling of tissue slices via histology- in whole organs. Collectively, the imaging of *T. cruzi* in clarified tissues also affords new appreciation of the morphology of infected cells, the variability in distribution of infected cells within tissues and the heavy bias for infection of muscle cells in the various tissues and provides a method to study strain variability, drug sensitivity, tissue distribution and immune response in this and other host:pathogen interactions.

Materials and Methods

Study Design

In this study we have developed and evaluated a long-term but less-intensive drug-sparing BNZ treatment protocol that provides 100% cure rates in mice chronically infected with *T. cruzi*. The determination of treatment efficacy was assessed by flow cytometry, qPCR, hemocultures and whole-body luciferase imaging. Additionally, we established tissue clearing and light-sheet fluorescent microscopy (LSFM) methods that allow the quantification of actively replicating and dormant parasites in whole tissues/organs. Details

regarding these techniques are available below. Female and male mice, 8-12 weeks old were used for infections throughout the study. The sample size and infection dose are provided in each figure legends. Samples size was determined based upon our knowledge of heterogeneity in parasite burden during *T. cruzi* infection and published reports using similar experimental strategies. Data collected were included if productive *T. cruzi* infection was established (visualized by luciferase imaging or flow cytometry by detection of *T. cruzi*-tetramer specific $CD8^+$ T cells). The investigators were not blinded during the collection or analysis of data and mice were randomly assigned to treatment groups prior to the start of each experiment.

Mice, parasites and infections

C57BL/6J (Stock No:000664) mice (C57BL/6 wild-type) were purchased from The Jackson Laboratory (Bar Harbor, ME) and C57BL/6J-IFN-γ knockout mice (also known as B6.129S7-Ifngtm1Ts/J - The Jackson Laboratory stock No 002287) (IFN-gamma deficient) were bred in-house at the University of Georgia Animal Facility. All the animals were maintained in the University of Georgia Animal Facility under specific pathogen-free conditions. *T. cruzi* tissue culture trypomastigotes of the wild-type strains Brazil, Colombiana and ARC-0704 were maintained through passage in Vero cells (American Type Culture Collection (Manassas, VA)) cultured in RPMI 1640 medium with 10% fetal bovine serum at 37°C in an atmosphere of 5% CO_2. Also, in this study we use the Brazil strain expressing eGFP and the Colombiana strain co-expressing firefly luciferase and tdTomato reporter proteins generated as described previously (9, 31) . Mice were infected subcutaneously in the footpad, intraperitoneally or intramuscularly with tissue culture trypomastigotes of *T. cruzi* and euthanized by carbon dioxide inhalation. This study was carried out in strict accordance with the Public Health Service Policy on Humane Care and Use of Laboratory Animals and Association for Assessment and Accreditation of Laboratory Animal Care accreditation guidelines. The protocol was approved by the University of Georgia Institutional Animal Care and Use Committee.

Drug treatment and in vivo imaging

Infected mice were treated according to the indicated schedules. Benznidazole (BNZ – Elea Phoenix,) was prepared by pulverization of tablets followed by suspension in an aqueous solution of 1% sodium carboxymethylcellulose with 0.1% Tween 80 and delivered orally by gavage at a concentration dosage of 100, 250 or 500mg/kg body weight. Each mouse received 0.2 ml of this suspension. Luciferase-expressing parasites were quantified in mice by bioluminescent detection. Mice were injected intraperitoneally with D-luciferin (150 mg/kg; PerkinElmer,) and anesthetized using 2.5% (vol/vol) gaseous isofluorane in oxygen prior to imaging on an IVIS Lumina II imager (Xenogen,) as previously described (32). Quantification of bioluminescence and data analysis was performed using Living Image v4.3 software (Xenogen,). Exposure time was 5 minutes.

T-cell phenotyping

Mouse peripheral blood was obtained by retro-orbital venipuncture, collected in sodium citrate solution, red blood cells lysed and the remaining cells were washed in staining buffer (2% BSA, 0.02% azide in PBS (PAB)) as previously described (10). Whole blood was

incubated with a major histocompatibility complex I (MHC I) tetramer containing the specific TSKB20 peptide (ANYKFTLV/Kb) labeled with BV421 (Tetramer Core Facility at Emory University, Atlanta, GA) and the following labeled antibodies: anti-CD8 FITC, anti-CD4 APC EF780, anti-CD127 PE (BD Bioscience,). For whole blood, we lysed red blood cells in a hypotonic ammonium chloride solution after washing twice in PAB. We stained cells for 45 min at 4°C in the dark, washed them twice in PAB and fixed them in 2% formaldehyde. At least 500,000 cells were acquired using a CyAn ADP flow cytometer (Beckman Coulter,) and analyzed with FlowJo software v10.6.1 (Treestar, Inc.).

In vitro maximal luminescence ATP detection assay

T. cruzi epimastigotes from the ARC-0704 strain were used in this assay. Parasites were isolated from tissue culture or hemocultures at 77 weeks from mice untreated or treated with 100mg/kg of BNZ and submitted to termination of the treatment at week 55. Approximately 25,000 log-phased epimastigotes were subjected to serial 2-fold dilutions of BNZ starting at 80 μM for 4 days before measuring their ATP production using ATPlite™ Luminescence ATP Detection Assay System (PerkinElmer,). Luminescence was read using BioTek Synergy Hybrid Multi-Mode reader (BioTek,). A dose response curve was generated with GraphPad Prism 5.0, (GraphPad Software, Inc.). IC50 was determined as the drug concentration that was required to inhibit 50% of ATP production compared to that of parasites with no drug exposure.

Quantitative polymerase chain reaction and hemoculture

Mouse tissue samples of skeletal muscle, heart, intestine and adipose tissue were collected at various time points and processed for quantification of *T. cruzi* DNA by real-time quantitative polymerase chain reaction (qPCR). DNA from mouse tissues was extracted using the protocol included with the Qiagen DNeasy Blood and Tissue Kit (Qiagen). Following the spin-column protocol for “Purification of Total DNA from Animal Tissues”, approximately 100μl piece of tissue from the desired animal was minced finely using micro-dissecting scissors (Millipore Sigma) and proceed with the extraction protocol as described by the manufacturer. All DNA samples were diluted to 25 ng/μl in nuclease free water. The generation of PCR standards and detection of parasite tissue load by qPCR was carried out as previously described (10, 18, 33). For the qPCR reactions we used the *T. cruzi* primers S35 (AAATAATGTACGGGKGAGATGCATGA) and S36 (GGGTTGGATTGGGGTTGGTGT) as well as tumor necrosis factor (TNF) housekeeping genes primers 5411 (CAGCAAGCATCTATGCACTTAGACCCC) and 5241(TCCCTCTCATCAGRRCTATGGCCCA). qPCR reactions consisted of 50 ng of genomic DNA; 0.5 μM of each primer set along with 10μl IQ SYBR green and water to make a 20μl final volume reaction. C1000 touch Bio rad CFX96 real time PCR detection system was used under the following cycling conditions: 1. Initial Denaturation 95°, 10 minutes. 2. Denaturation 95°C, 15 seconds. 3. Annealing 60°C, 15 seconds. 4. Extension 72°C, 15 seconds. 5. Plate read. 6. x40 cycles. 7. 95°C, 1 second. 8. Melt curve creation 60-93°C, 30 seconds, 0.5°C/cycle. Lid 105°C. The range of standards for these particular assays was 1.7×10^{2}-1.7×10^{-3}. For each tissue type a TNF reference was included matching that tissue type. A two-fold serial dilution was used to create 8 standards for TNF comparison. Analysis of the data was done using a BioRad CFX manager software version

3.1 (BioRad,). Samples were analyzed by looking at the starting quantity (SQ) mean value for each replicate and making an average of 2 replicates per mouse sample for both S35/36 and TNF primer reactions. S35/36 SQ mean values were compared to the S35/36 standard curve while the TNF SQ mean values were compared to the TNF standard curve for each respective plate. The S35/36 average SQ mean value was then divided by the TNF average SQ mean value and multiplied by 50 to reach the parasite equivalence per 50 ng of DNA. The limit of detection was set at the lowest standard .0017. For hemocultures determinations, peripheral blood from infected mice was collected and cultured at 26°C in supplemented liver digest neutralized tryptose (LDNT) medium as described previously (34). The presence of *T. cruzi* parasites was assessed every week for 3 months under inverted microscope.

Tissue clearing

Multiple tissue clearing protocols were tested (SCALE, CLARITY, uDISCO, iDISCO, vDISCO and FDISCO) however; tdTomato or eGFP parasite fluorescence was best preserved using the **c**lear, **u**nobstructed **b**rain or body **i**maging **c**ocktails (CUBIC). All the tissue clearings performed in this work were done using CUBIC protocol I (20). We use three different cocktails: CUBIC-P for delipidation and rapid decolorization: 5 wt% 1-methylimidazole, 10 wt% *N*-butyldiethanolamine, 5 wt% Triton X-100; CUBIC-L for delipidation and decolorization: 10 wt% *N*-butyldiethanolamine, 10 wt% Triton X-100 and CUBIC-R for refractive index (RI) matching: 10 wt% 1,3-bis(aminomethyl)cyclohexane, 10 wt% sodium dodecylbenzenesulfonate, pH 12.0 adjusted by *p*-toluenesulfonic acid. Mice (C57BL/6 wild-type and IFN-gamma-deficient) were euthanized by carbon dioxide inhalation. As soon as the animals did not show any pedal reflex, they were intracardially perfused with 50 ml of PBS (pH 7.4); 50 ml of 4% (w/v) paraformaldehyde (PFA) in PBS and 100 ml of CUBIC-P cocktail. After perfusions, the organs were dissected and immersed individually in 10ml of 1:1 water-diluted CUBIC-L using 50ml falcon tubes (ThermoFisher Scientific,) in an orbital shaker (150rpm) at 37°C overnight. The next day tissues were immersed in 10ml of 100% CUBIC-L for 6 days (refreshing the solution on day three) and washed with 30 ml of 1x PBS overnight shaking at room temperature. To avoid tissue damage, organs were maintained in the same tube during the complete protocol and solutions were collected using a vacuum system. The organs were then immersed in 1:1 water-diluted CUBIC-R solution with shaking (150rpm) at room temperature overnight and then immersed in 100% CUBIC-R with shaking (150rpm) at room temperature for 2-3 days. To eliminate bubbles inside the heart and/or tissue surfaces, CUBIC-R solution was carefully dried out using cleaning wipes (Kimwipes, Kimberly-Clark,) and then incubated in 10ml of immersion oil (RI =1.51, Cargille laboratories) using 6-wells cell culture plates (ThermoFisher Scientific). The next day remaining bubbles were discarded by using tweezers. Organs were adhering to a flat-top sample holder (LaVision BioTec) by using cyanoacrylate-based gel superglue (Scotch). Whole organs were imaged transversally to their longitudinal axis. Hearts were glued with the apex and the aorta horizontally aligned. For image acquisition, cleared samples were immersed in 100-120ml of immersion oil in a quartz cuvette and prepared for LSFM imaging.

Light-sheet fluorescent microscopy and image processing

CUBIC transparent organs were imaged in 3D using a Ultramicroscope II imaging system and ImSpector software (both from LaVision BioTec,). This Light-Sheet Microscope was equipped with an Olympus MVX10 Zoom Body (Olympus,), a LaVision BioTec Laser Module with 488 nm, 561 nm, 640 nm, and 785 nm lasers lines, and an Andor Neo sCMOS Camera with a pixel size of 6.5 × 6.5 μm^2. Organs were imaged at 1.26x using right and left light sheets (3 on each side) lasers with 5μm thickness and 100% width. The exposure time was kept constant at 50 milliseconds (ms) and the laser power was adjusted from 10% to 80% depending on the intensity of the fluorescence signal. Stepsize between individual slices was adjusted to 3μm. A variable number of TIFF images were obtained depending on organ size ranging from 300-1500. TIFF stacks were converted (ImarisFileConverterx64, v9.2.0, BitPlane, AG) into Imaris files (.ims). 3D reconstruction and subsequent analysis was done using Imaris software v9.3 (Bitplane AG,). Movies were generated by Imaris using a total of 800 frames reproduced at 24 frames per second (fps). 2D slice animations were generated by the orthoslicer Imaris software tool and reproduced at 24fps. Movies were edited and transcoded by the open-source software OpenShot v2.5.1 (OpenShot Studios,) and HandBrake v1.3.1 (The HandBrake Team,), respectively. Supplemental Movies were strongly downsampled to accommodate the large original datasets. The loss of optical image quality in the movies was kept at a minimum; however, it was impossible to avoid completely.

Automated parasite quantification

For the quantification of parasite nests and dormant parasites appropriate threshold of signals from reporter proteins was selected in each experiment. Automatic cell counting tool under the spot detection algorithm was performed using Imaris software. An initial analysis was performed in a randomly selected 3D ROI and then applied to the entire 3D organ reconstruction. For the automated counting of amastigote nests, we select 532nm channel and then count elongated forms with up to 200μm radius distance. To identify DiR near-infrared positive dormant parasites, we selected the 639nm channel to count cells of 3-5μm radius distance. Artifacts within tissues are usually bright in multiple channels. We take advantage of this property to discard artifacts by imaging using an additional channel (often 488nm channel). Double color objects (GFP/tdTomato or GFP/DiR near-infrared) were considered artifacts and not considered for counting.

Confocal laser-scanning microscopy imaging

Confocal fluorescence imaging was performed using a Zeiss LSM 710 inverted confocal microscope attached to an EXFO Xcite series 120Q lamp and a digital Zeiss XM10 camera (Carl Zeiss AG). For LSFM validation experiments, a transparent section of the heart was placed on a 35 mm glass-bottom petri dish and mounted in a drop of immersion oil before imaging using 10x and 100x objectives. The peritoneal adipose tissue was placed over a surface of ~1.6 cm^2 and the skeletal muscle was sliced into thin sections and mounted using ProLong Diamond anti-fade solution (ThermoFisher Scientific). Tissue slices were exhaustively scanned and the images were taken using 63x objectives. A Zeiss Zen software was used to process the optical z-stack sections into a single 2D image.

Labelling of parasites with fluorescent dyes

Cell suspensions of *T. cruzi* trypomastigotes were labeled with the near-infrared fluorescent cyanine dye DiR ($DiIC_{18}(7)$;1,1′-dioctadecyl-3,3,3′,3′-tetramethylindotricarbocyanine iodide) (Biotium,) following manufacturer's instructions. Briefly, 1×10^6 trypomastigotes were incubated for 20 min at 37°C with 2μg/mL DiR, protected from light. Unbound dye was quenched by the addition of five volumes of 1x PBS. After an additional washing in warm FBS-RPMI, parasites were used for infection of cell cultures or mice. For DiR and CellTrace Far Red co-staining, 1×10^6 trypomastigotes were incubated for 20 min at 37°C with 2μg/mL DiR and 10 μM CellTrace Far Red (CellTrace Cell Far Red Proliferation Kit, ThermoFisher Scientific), protected from light. The quenching of unbound dyes was performed as previously described.

Statistical analysis

The Mann-Whitney U tests and one-way variance analysis (ANOVA) of the GraphPad Prism version 5.0 software were used. Values are expressed as means ± standard error of mean of at least three separate experiments. P values equal to or less than 0.05 were considered significant.

Supplementary Material

Refer to Web version on PubMed Central for supplementary material.

Acknowledgements:

We are grateful to Julie Nelson from the CTEGD Flow cytometry core and Muthugapatti Kandasamy from the Biomedical Microscopy Core for their technical support. We also would like to thank HuiFeng Shen, Ashley Driver and Dylan Orr for their skillful technical assistance in this work and all the members of Tarleton Research Group for helpful suggestions throughout this study. Etsuo A. Susaki from the University of Tokyo is acknowledged for his valuable help regarding tissue clearing protocols.

Funding: This work was supported by US National Institutes of Health grants R01 AI124692 to RLT and R21 AI142469 and to RLT and JMB.

References

1. Schofield CJ, Jannin J, Salvatella R, The future of Chagas disease control. Trends Parasitol 22, 583–588 (2006). [PubMed: 17049308]
2. Hotez PJ, Molyneux DH, Fenwick A, Kumaresan J, Sachs SE, Sachs JD, Savioli L, Control of neglected tropical diseases. N Engl J Med 357, 1018–1027 (2007). [PubMed: 17804846]
3. WHO, Chagas disease in Latin America: an epidemiological update based on 2010 estimates. WHO Weekly Epidemiological Record (WER) 90, 33–44 (2015).
4. Rodriques Coura J, de Castro SL, A critical review on Chagas disease chemotherapy. Memorias do Instituto Oswaldo Cruz 97, 3–24 (2002). [PubMed: 11992141]
5. Urbina JA, Specific chemotherapy of Chagas disease: relevance, current limitations and new approaches. Acta tropica 115, 55–68 (2010). [PubMed: 19900395]
6. Viotti R, Vigliano C, Lococo B, Alvarez MG, Petti M, Bertocchi G, Armenti A, Side effects of benznidazole as treatment in chronic Chagas disease: fears and realities. Expert Rev Anti Infect Ther 7, 157–163 (2009). [PubMed: 19254164]
7. Alvarez MG, Hernandez Y, Bertocchi G, Fernandez M, Lococo B, Ramirez JC, Cura C, Albizu CL, Schijman A, Abril M, Sosa-Estani S, Viotti R, New Scheme of Intermittent Benznidazole Administration in Patients Chronically Infected with Trypanosoma cruzi: a Pilot Short-Term

Follow-Up Study with Adult Patients. Antimicrobial agents and chemotherapy 60, 833–837 (2016). [PubMed: 26596935]

8. Alonso-Padilla J, Cortes-Serra N, Pinazo MJ, Bottazzi ME, Abril M, Barreira F, Sosa-Estani S, Hotez PJ, Gascon J, Strategies to enhance access to diagnosis and treatment for Chagas disease patients in Latin America. Expert Rev Anti Infect Ther 17, 145–157 (2019). [PubMed: 30712412]
9. Sanchez-Valdez FJ, Padilla A, Wang W, Orr D, Tarleton RL, Spontaneous dormancy protects Trypanosoma cruzi during extended drug exposure. Elife 7, (2018).
10. Bustamante JM, Craft JM, Crowe BD, Ketchie SA, Tarleton RL, New, combined, and reduced dosing treatment protocols cure Trypanosoma cruzi infection in mice. The Journal of infectious diseases 209, 150–162 (2014). [PubMed: 23945371]
11. Barrett MP, Kyle DE, Sibley LD, Radke JB, Tarleton RL, Protozoan persister-like cells and drug treatment failure. Nat Rev Microbiol 17, 607–620 (2019). [PubMed: 31444481]
12. Aldasoro E, Posada E, Requena-Mendez A, Calvo-Cano A, Serret N, Casellas A, Sanz S, Soy D, Pinazo MJ, Gascon J, What to expect and when: benznidazole toxicity in chronic Chagas' disease treatment. J Antimicrob Chemother 73, 1060–1067 (2018). [PubMed: 29351667]
13. Castro JA, de Mecca MM, Bartel LC, Toxic side effects of drugs used to treat Chagas' disease (American trypanosomiasis). Hum Exp Toxicol 25, 471–479 (2006). [PubMed: 16937919]
14. Marinho CR, Nunez-Apaza LN, Martins-Santos R, Bastos KR, Bombeiro AL, Bucci DZ, Sardinha LR, Lima MR, Alvarez JM, IFN-gamma, but not nitric oxide or specific IgG, is essential for the in vivo control of low-virulence Sylvio X10/4 Trypanosoma cruzi parasites. Scand J Immunol 66, 297–308 (2007). [PubMed: 17635807]
15. Ferraz ML, Gazzinelli RT, Alves RO, Urbina JA, Romanha AJ, The Anti-Trypanosoma cruzi activity of posaconazole in a murine model of acute Chagas' disease is less dependent on gamma interferon than that of benznidazole. Antimicrobial agents and chemotherapy 51, 1359–1364 (2007). [PubMed: 17220408]
16. Andrade SG, Magalhaes JB, Pontes AL, Evaluation of chemotherapy with benznidazole and nifurtimox in mice infected with Trypanosoma cruzi strains of different types. Bull World Health Organ 63, 721–726 (1985). [PubMed: 3936634]
17. Martins HR, Figueiredo LM, Valamiel-Silva JC, Carneiro CM, Machado-Coelho GL, Vitelli-Avelar DM, Bahia MT, Martins-Filho OA, Macedo AM, Lana M, Persistence of PCR-positive tissue in benznidazole-treated mice with negative blood parasitological and serological tests in dual infections with Trypanosoma cruzi stocks from different genotypes. J Antimicrob Chemother 61, 1319–1327 (2008). [PubMed: 18343804]
18. Bustamante JM, Bixby LM, Tarleton RL, Drug-induced cure drives conversion to a stable and protective $CD8^+$ T central memory response in chronic Chagas disease. Nat Med 14, 542–550 (2008). [PubMed: 18425131]
19. Bixby LM, Tarleton RL, Stable $CD8^+$ T cell memory during persistent Trypanosoma cruzi infection. J Immunol 181, 2644–2650 (2008). [PubMed: 18684955]
20. Tainaka K, Murakami TC, Susaki EA, Shimizu C, Saito R, Takahashi K, Hayashi-Takagi A, Sekiya H, Arima Y, Nojima S, Ikemura M, Ushiku T, Shimizu Y, Murakami M, Tanaka KF, Iino M, Kasai H, Sasaoka T, Kobayashi K, Miyazono K, Morii E, Isa T, Fukayama M, Kakita A, Ueda HR, Chemical Landscape for Tissue Clearing Based on Hydrophilic Reagents. Cell Rep 24, 2196–2210 e2199 (2018). [PubMed: 30134179]
21. Pampaloni F, Chang BJ, Stelzer EH, Light sheet-based fluorescence microscopy (LSFM) for the quantitative imaging of cells and tissues. Cell Tissue Res 360, 129–141 (2015). [PubMed: 25743693]
22. Swoger J, Pampaloni F, Stelzer EH, Light-sheet-based fluorescence microscopy for three-dimensional imaging of biological samples. Cold Spring Harb Protoc 2014, 1–8 (2014). [PubMed: 24371323]
23. Francisco AF, Lewis MD, Jayawardhana S, Taylor MC, Chatelain E, Kelly JM, Limited Ability of Posaconazole To Cure both Acute and Chronic Trypanosoma cruzi Infections Revealed by Highly Sensitive In Vivo Imaging. Antimicrobial agents and chemotherapy 59, 4653–4661 (2015). [PubMed: 26014936]

24. Torrico F, Gascon J, Ortiz L, Alonso-Vega C, Pinazo MJ, Schijman A, Almeida IC, Alves F, Strub-Wourgaft N, Ribeiro I, Group ES, Treatment of adult chronic indeterminate Chagas disease with benznidazole and three E1224 dosing regimens: a proof-of-concept, randomised, placebo-controlled trial. Lancet Infect Dis 18, 419–430 (2018). [PubMed: 29352704]
25. Assiria Fontes Martins T, de Figueiredo Diniz L, Mazzeti AL, da Silva do Nascimento AF, Caldas S, Caldas IS, de Andrade IM, Ribeiro I, Bahia MT, Benznidazole/Itraconazole Combination Treatment Enhances Anti-Trypanosoma cruzi Activity in Experimental Chagas Disease. PLoS One 10, e0128707 (2015). [PubMed: 26076455]
26. Mazzeti AL, Diniz LF, Goncalves KR, WonDollinger RS, Assiria T, Ribeiro I, Bahia MT, Synergic Effect of Allopurinol in Combination with Nitroheterocyclic Compounds against Trypanosoma cruzi. Antimicrobial agents and chemotherapy 63, (2019).
27. Moreira da Silva R, Oliveira LT, Silva Barcellos NM, de Souza J, de Lana M, Preclinical monitoring of drug association in experimental chemotherapy of Chagas' disease by a new HPLC-UV method. Antimicrobial agents and chemotherapy 56, 3344–3348 (2012). [PubMed: 22450981]
28. Perin L, Moreira da Silva R, Fonseca KD, Cardoso JM, Mathias FA, Reis LE, Molina I, Correa-Oliveira R, Vieira PM, Carneiro CM, Pharmacokinetics and Tissue Distribution of Benznidazole after Oral Administration in Mice. Antimicrobial agents and chemotherapy 61, (2017).
29. Canavaci AM, Bustamante JM, Padilla AM, Perez Brandan CM, Simpson LJ, Xu D, Boehlke CL, Tarleton RL, In vitro and in vivo high-throughput assays for the testing of anti-Trypanosoma cruzi compounds. PLoS neglected tropical diseases 4, e740 (2010). [PubMed: 20644616]
30. Khare S, Nagle AS, Biggart A, Lai YH, Liang F, Davis LC, Barnes SW, Mathison CJ, Myburgh E, Gao MY, Gillespie JR, Liu X, Tan JL, Stinson M, Rivera IC, Ballard J, Yeh V, Groessl T, Federe G, Koh HX, Venable JD, Bursulaya B, Shapiro M, Mishra PK, Spraggon G, Brock A, Mottram JC, Buckner FS, Rao SP, Wen BG, Walker JR, Tuntland T, Molteni V, Glynne RJ, Supek F, Proteasome inhibition for treatment of leishmaniasis, Chagas disease and sleeping sickness. Nature 537, 229–233 (2016). [PubMed: 27501246]
31. Peng D, Kurup SP, Yao PY, Minning TA, Tarleton RL, CRISPR-Cas9-mediated single-gene and gene family disruption in Trypanosoma cruzi. mBio 6, e02097–02014 (2014). [PubMed: 25550322]
32. Canavaci A, Bustamante J, Padilla A, Perez Brandan C, Simpson L, Xu D, Boehlke C, Tarleton R, In vitro and in vivo high-throughput assays for the testing of anti-Trypanosoma cruzi compounds. PLoS Negl Trop Dis 4, (2010).
33. Cummings KL, Tarleton RL, Rapid quantitation of Trypanosoma cruzi in host tissue by real-time PCR. Molecular and biochemical parasitology 129, 53–59 (2003). [PubMed: 12798506]
34. Xu D, Brandan CP, Basombrio MA, Tarleton RL, Evaluation of high efficiency gene knockout strategies for Trypanosoma cruzi. BMC Microbiol 9, 90 (2009). [PubMed: 19432966]

Editor's summary:

Trouncing trypanosomes

Trypanosoma cruzi infection causes Chagas disease in millions of individuals in Latin America, and intensive drug treatment is frequently unsuccessful. Bustamante *at al.* demonstrated that high weekly doses of oral benznidazole over 30 weeks, rather than the current treatment of smaller twice daily doses over 2 months, resulted in better clearance of both actively replicating and dormant trypanosomes in mouse models of Chagas disease. The clearance of dormant parasites was confirmed by light sheet fluorescence microscopy, which allowed the authors to image whole organs and intact tissues of infected mice. Further studies will determine if this drug regimen will be successful for treating those with Chagas disease.

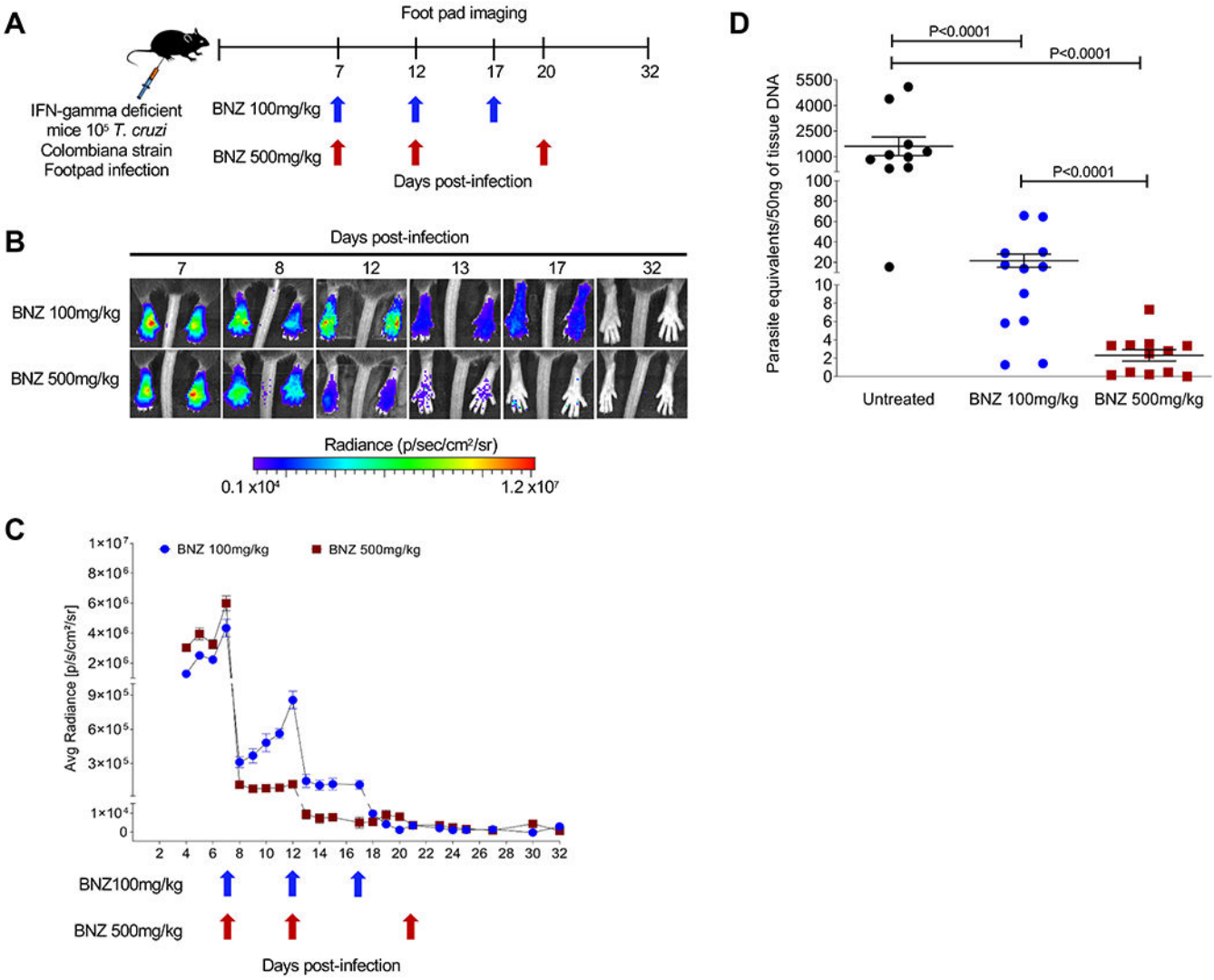

Fig. 1. Effect of varying the frequency and dosage of BNZ administration on the control of *T. cruzi* infection in mice.

(A) Schematic of infection, treatment and footpad imaging. IFN-gamma deficient mice (5 mice in each group) were infected in the footpads with 10^5 trypomastigotes of the Luciferase-expressing Colombiana strain of *T. cruzi* and treated at indicated time points with either 100 or 500mg/kg oral BNZ. **(B)** Representative images showing footpad bioluminescent signal before and after treatment. The heat map is on a $\log_{10}$ scale and indicates the intensity of bioluminescence from low (blue) to high (red). **(C)** Parasite bioluminescence quantification following D-luciferin injection was measured at various times post-treatment in the footpads of mice infected and treated. Each data point represents the mean of 8 footpads bioluminescence from four mice expressed on a logarithmic scale. After subtraction of the background signal, the average radiance measurements (photons/second /cm^2/sr) were quantified. Data are shown as mean ± standard error of the mean. **(D)** *T. cruzi* DNA determined by quantitative real time polymerase chain reaction in footpads of untreated or treated mice at 12 days post-infection (5 days post-treatment). C57BL/6 wild-type mice (10-12 mice in each group) were infected in the footpads with 10^3

trypomastigotes of the Brazil strain of *T. cruzi* and left untreated or treated at day 2 post-infection with a single dose of BNZ at 100 or 500mg/kg concentration. A statistically significant difference was set at p=0.05.

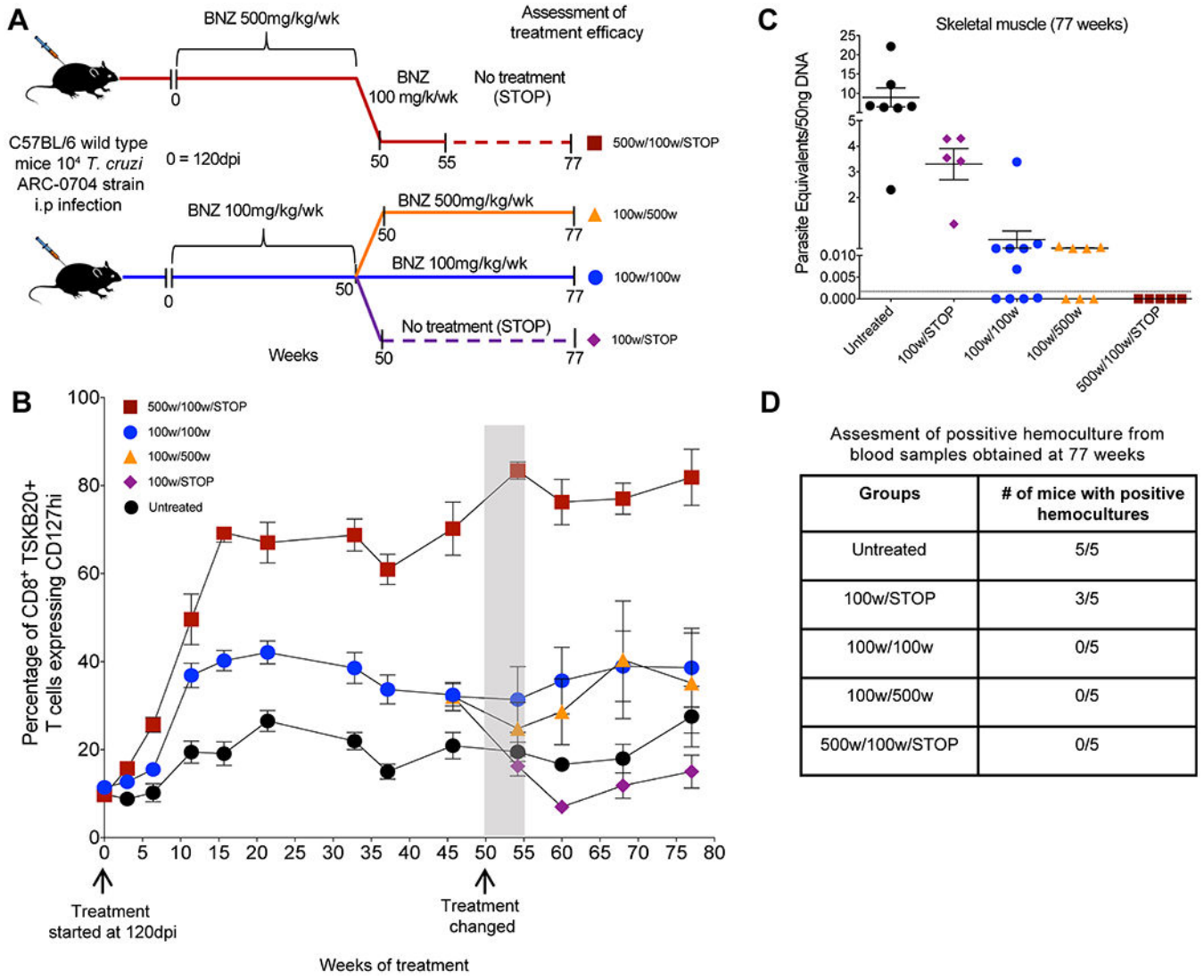

Groups	# of mice with positive hemocultures
Untreated	5/5
100w/STOP	3/5
100w/100w	0/5
100w/500w	0/5
500w/100w/STOP	0/5

Fig. 2. A weekly BNZ treatment regimen of 500 mg/kg cures mice chronically infected with *T. cruzi*.

(A) Schematic of infection, treatment and assessment of treatment efficacy. C57BL/6 wild-type mice (14-15 mice in each group) were infected intraperitoneally with 10^4 trypomastigotes of the ARC-0704 strain of *T. cruzi* and left untreated or treated weekly, starting at 120 days post-infection, with BNZ at 100 or 500mg/kg concentration over 50 weeks. At 50 weeks of treatment mice treated with 500mg/kg/wk were switched to a regimen of 100mg/kg/wk of BNZ from week 50 to 55, followed by a cessation of treatment at 55 weeks and termination of the experiment at week 77 (500w/100w/STOP). The mice receiving 100mg/kg/wk of BNZ were divided in three groups on week 50 of treatment; one group was switched to a 500mg/kg/wk of BNZ until week 77 (100w/500w); a second group continued with the same regimen of 100mg/kg/wk of BNZ until week 77 (100w/100w), and in the third group the 100mg/kg/wk treatment was stopped at week 55 (100w/STOP). In all the groups the experiment was terminated at 77 weeks of treatment. **(B)** Expression of the T_{cm} marker CD127 in blood on $CD8^+$ TSKB20-tetramer$^+$ T cells from mice untreated and

undergoing different weekly treatment regimens. Data are shown as mean ± standard error of the mean. Arrows indicate the initiation of the treatment (120dpi= week 0) and week 50 where changes in the treatment regimens occurred for the treated groups (see description in A). The area in gray denotes 5 weeks corresponding to weeks 50-55 where the mice previously treated with BNZ at 500mg/kg/wk were switched to 100mg/kg/wk (see description in A). **(C)** *T. cruzi* DNA isolated from skeletal muscle of untreated or treated mice at 77 weeks from experiment depicted in (A-B) and assayed by qPCR. A statistically significant difference was set at p=0.05. **(D)** Blood from these mice collected at 77 weeks was submitted to hemoculture assays and analyzed for parasite growth for >60 days.

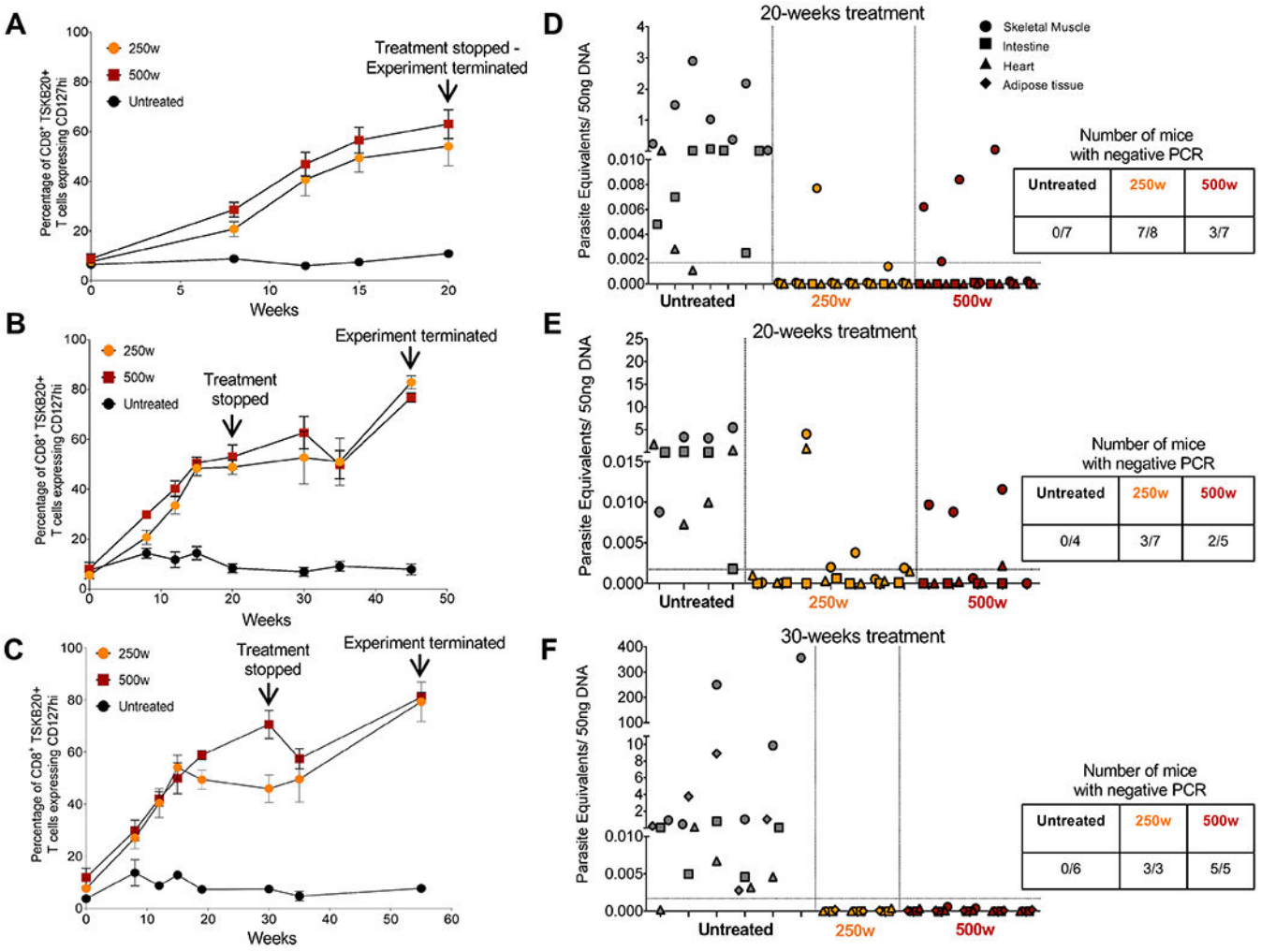

Fig. 3. Curative effects of BNZ of weekly dosing using 2.5X - 5X the standard daily dose in chronic *T. cruzi* infection.

C57BL/6 wild-type mice (3-8 mice in each group) were infected intraperitoneally with 10^4 trypomastigotes of the Colombiana strain of *T. cruzi* and left untreated or treated weekly, starting at 180 days post-infection (day 0), with BNZ at 250 or 500mg/kg concentration over 20 (**A, B, D, and E**) or 30 weeks (**C and F**). Treatment was stopped at week 20 or 30 and assessment of treatment efficacy was carried out at week 20, 45 or 55 as indicated. (**A-C**) Expression of the T_{cm} marker CD127 on blood $CD8^+$ TSKB20-tetramer+ T cells from mice untreated and treated with BNZ at 250 or 500mg/kg/wk. Data are shown as mean ± standard error of the mean. (**D-F**) Detection of *T. cruzi* DNA in samples of skeletal muscle, intestine, heart and adipose tissue of untreated or treated mice at 20, 45 and 55 weeks and assayed by qPCR. Each x-axis hash marks tissues from an individual animal.

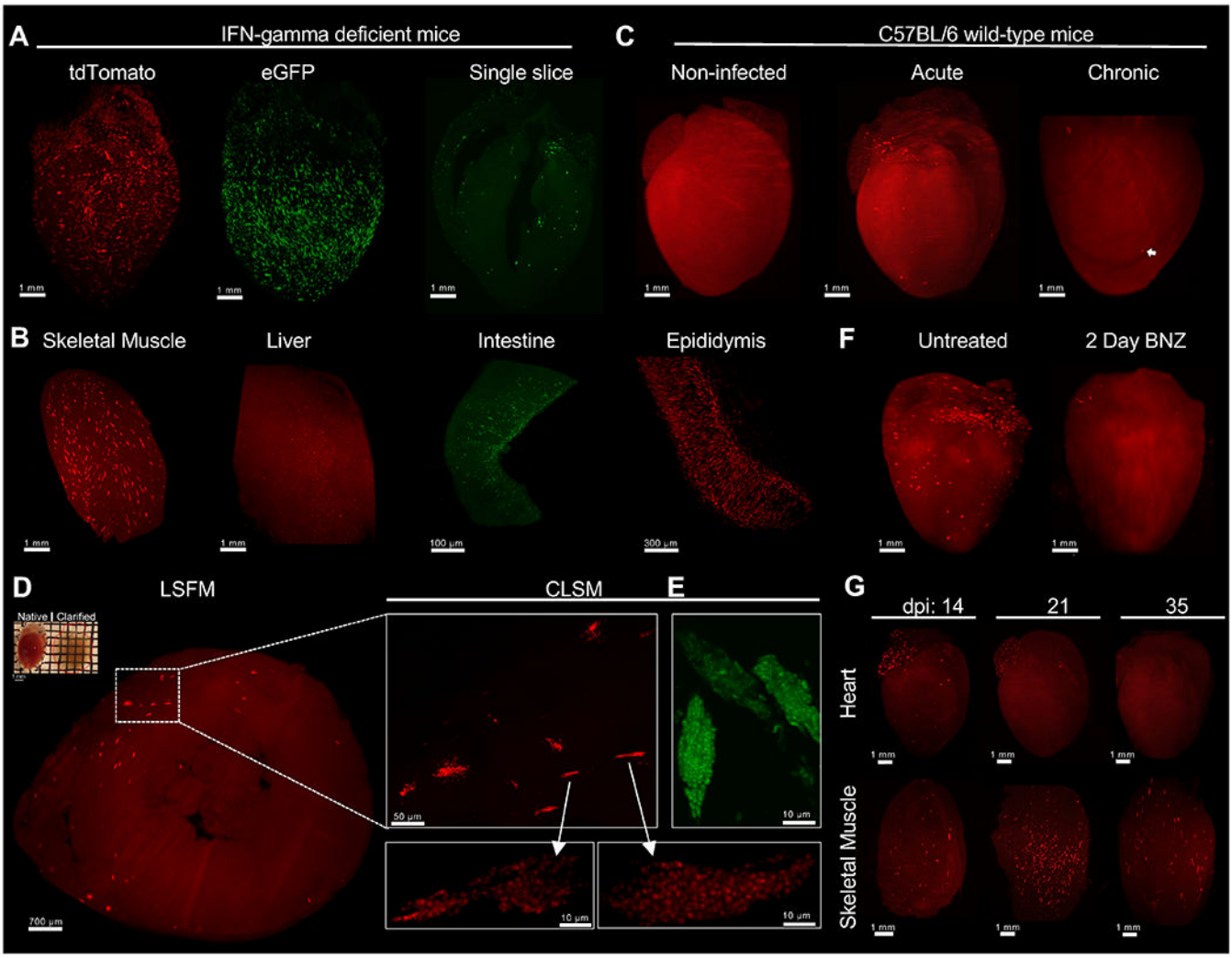

Fig. 4. Light-sheet fluorescence microscopy enables *T. cruzi* infection tracking in whole-organs after CUBIC tissue clarification.

C57BL/6 wild-type or IFN-gamma-deficient mice were intraperitoneally infected with 2 ×10^5 *T. cruzi* tdTomato-expressing Colombiana or eGFP-expressing Brazil strains. At different time points, mice were euthanized, perfused with PBS, PFA and CUBIC clarifying cocktails. After organ collection, clarification was continued using CUBIC reagents and finally prepared for LSFM imaging. **(A and B)** 3D reconstruction of IFN-gamma-deficient mice organs infected with tdTomato-expressing Colombiana (red) or eGFP-expressing Brazil (green) *T. cruzi* strains in the acute phase of the infection. A single optical slice of a clarified heart showing the detection of eGFP-expressing parasites (green) throughout the organ. Amastigote nests (bright red) can be differentiated from tissue-autofluorescence background (red). Low tissue autofluoresense was maintained to allow for the identification of complete organ morphology. **(C)** 3D reconstruction of the heart of C57BL/6 wild-type mice uninfected and infected with tdTomato-expressing Colombiana parasites in the acute and chronic phase of the infection. Arrow indicates an amastigote nest. **(D)** Confirmation of amastigote nests by confocal microscopy. A CUBIC-clarified heart from an acutely infected, IFN-gamma-deficient mouse (upper left) was sliced transversely in a 1mm slice and multiple

z-stack images were obtained by LSFM. Enlarged region of interest (ROI) shows nests containing tdTomato or **(E)** eGFP-expressing amastigotes and trypomastigotes using CLSM. **(F)** C57BL/6 wild-type mice infected with 2×10^5 tdTomato-expressing Colombiana strain trypomastigotes were left untreated or treated with 2 daily doses (on days 18 and 19 post infection) of BNZ at 100mg/kg concentration. On day 20 mice were euthanized, perfused and the heart was clarified and prepared for LSFM. **(G)** C57BL/6 wild-type mice were infected with 5×10^5 *T. cruzi* tdTomato-expressing Colombiana strain trypomastigotes. On day 14, 21 and 35 post-infection, mice were euthanized, skeletal muscle and heart were excised and clarified.

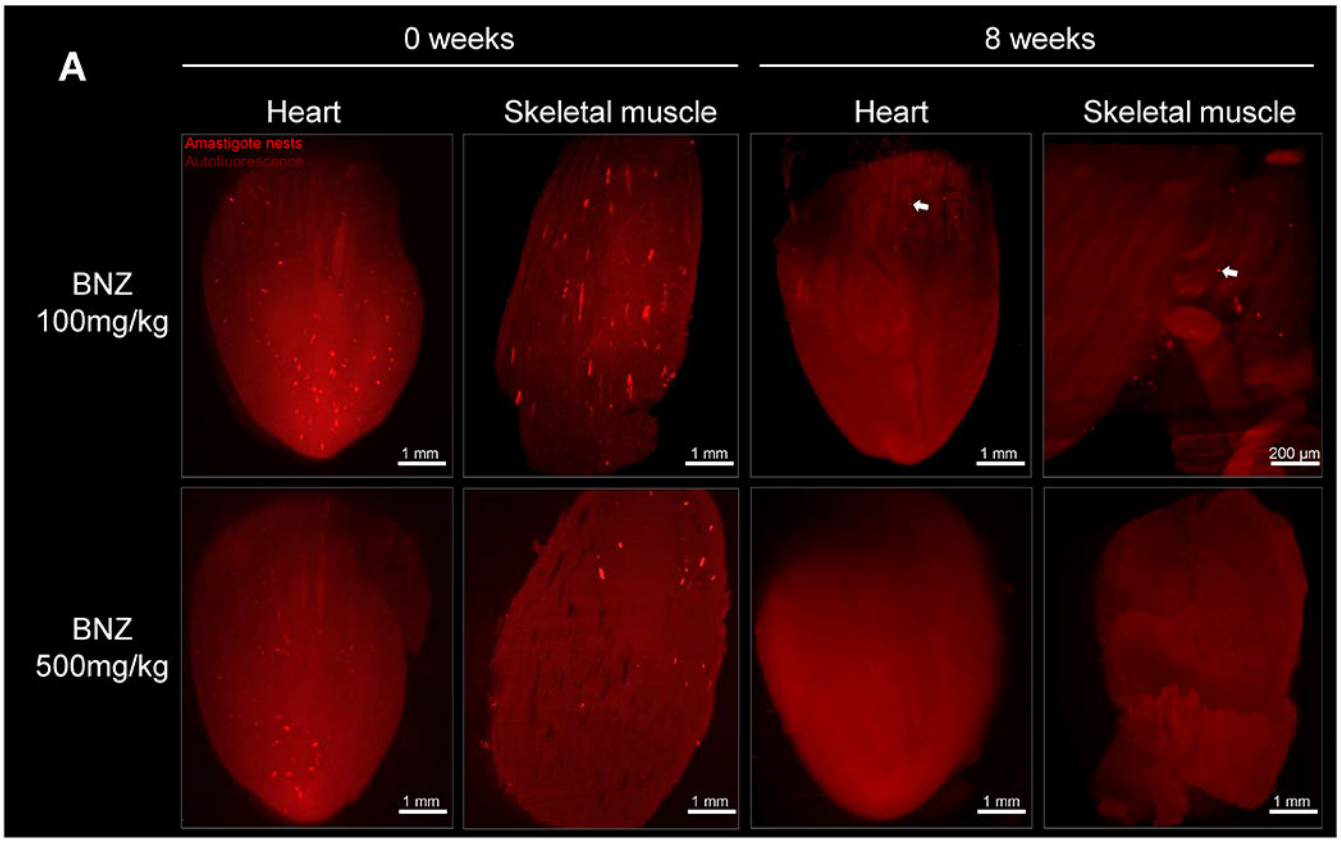

B

Parasite-infected cells detected at weeks post-treatment

		0	2	4	6	8
BNZ 100mg/kg	Heart	56	ND	1	2	5
	Muscle	79	2	5	3	6
BNZ 500mg/kg	Heart	64	ND	0	0	0
	Muscle	48	2	2	0	0

Fig. 5. Weekly doses of 500 mg/kg of BNZ is sufficient to eliminate *T. cruzi* in heart and skeletal muscle.

C57BL/6 wild-type mice were intraperitoneally infected with 4×10^6 tdTomato-expressing Colombiana trypomastigotes of *T. cruzi* and treated weekly for 7 weeks, with 100 or 500 mg/kg of BNZ, starting at 5 days post-infection. At each indicated time point, one mouse per group was sacrificed, perfused and heart and skeletal muscle were dissected, clarified and scanned using LSFM. **(A)** 3D reconstructions of heart and skeletal muscle showing amastigote nests (red) in untreated (0 weeks) and treated (8 weeks) mice. Arrows indicate amastigote nests. **(B)** Automated quantification of total *T. cruzi* amastigote nests in tissue 3D reconstructions. ND = not determined.

A Proliferating parasites

	Weeks				
	0	3	6	9	13
Untreated					
Heart	2.6	0.3	0	1	0
Muscle	24.6	27	11	2.3	1
Intestine	3.3	2.3	6	2.6	2
BNZ 500 mg/kg					
Heart	4	0	0	0	0
Muscle	29	4	0	0	0
Intestine	7	2.6	0	0	0

B Dormant parasites

	Weeks				
	0	3	6	9	13
Heart	1.3	2.3	0	0.6	0
Muscle	3	5	0.6	0.6	1
Intestine	11.3	4.6	2.3	0	0.6
Heart	9.6	0	0	0	0
Muscle	2.3	2.3	0	0	0
Intestine	8.3	5.6	0	0	0

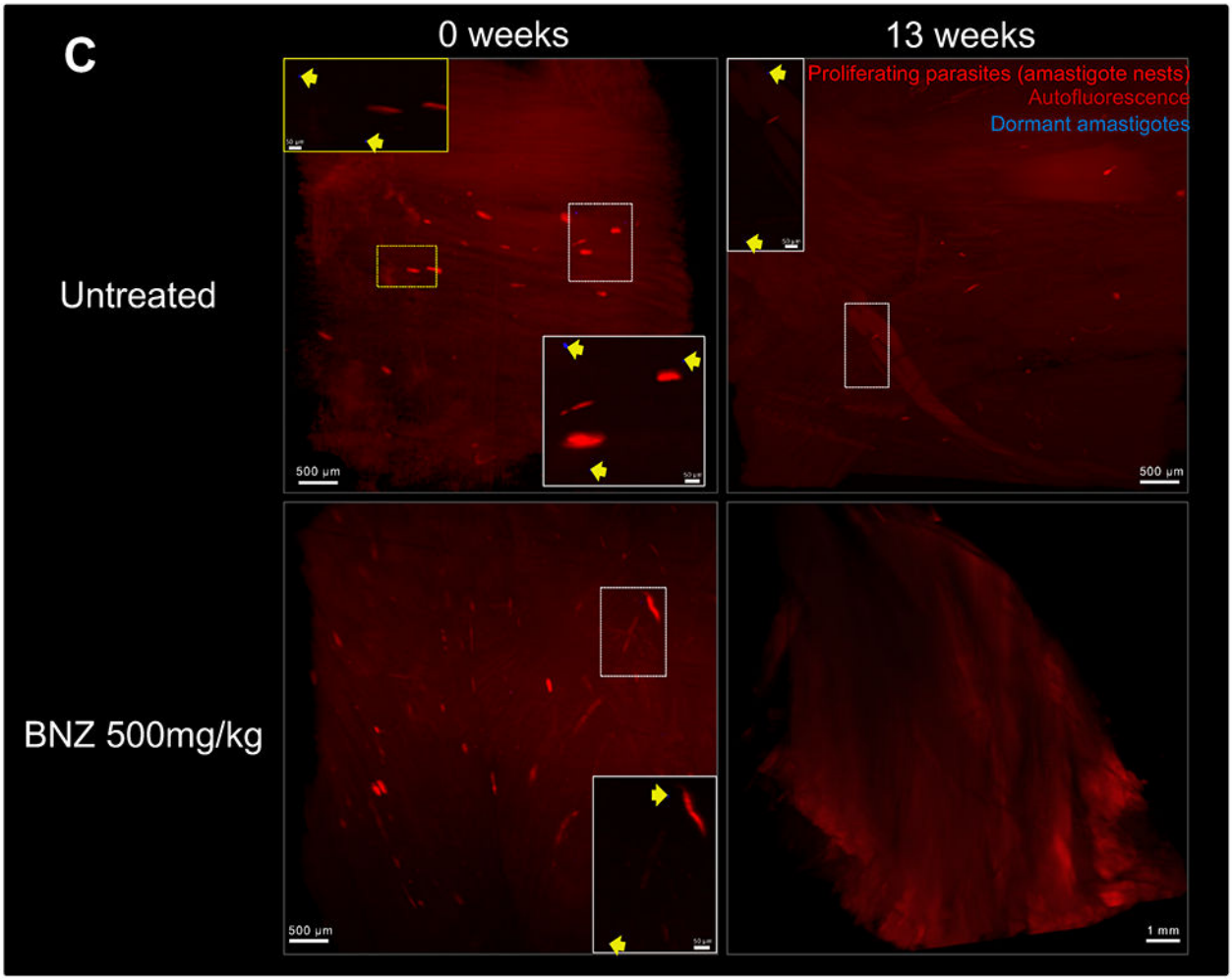

Fig. 6. Active and dormant parasites decline after weekly treatment with 500mg/kg of BNZ.

C57BL/6 wild-type mice (15 mice/group) were intraperitoneally infected with 4×10^6 trypomastigotes of the tdTomato-expressing Colombiana strain of *T. cruzi* stained with DiR near-infrared dye. Mice were untreated or treated weekly, starting 37 days post-infection, with BNZ at 500mg/kg concentration over 12 weeks. On weeks 0, 3, 6, 9 and 13, 3 mice per group were euthanized and perfused. After dissection of the heart, muscle and intestine tissues were clarified and scanned by LSFM. **(A)** Automated quantification of total tdTomato-positive parasite nests in 3D reconstructions of the heart, skeletal muscle and

intestine of mice untreated and treated with 500mg/kg of BNZ. The results correspond to the average number of nests in tissue samples from 3 individual mice (Table S1A). **(B)** Automated quantification of total DiR-positive dormant parasites. The results correspond to the average number of dormant parasites in tissue samples from 3 individual mice (Table S1B). **(C)** Representative 3D reconstructions of skeletal muscle showing tdTomato-positive parasite nests (red) and DiR-positive dormant individual amastigotes (blue) in untreated (0 weeks) and treated (13 weeks) mice. Yellow arrows indicate DiR-positive dormant amastigotes.